Biological Forum – An International Journal **15(6): 939-942(2023)**

ISSN No. (Print): 0975-1130
ISSN No. (Online): 2249-3239

Studies on the Structure and Antimicrobial Activity of $MgAl_2O_4:Tb^{3+}$ Nanophosphors Synthesized by Polymerised Sol-gel Method

Deepa Rani S.[1]*, Sajan P. Shamsudeen[2] and Abhilash Kumar R.G.[1]
[1]Department of Physics, Government College for Women, Thiruvananthapuram (Kerala), India.
[2]Department of Physics, University College, Thiruvananthapuram (Kerala), India.

(Corresponding author: Deepa Rani S.)*
(Received: 04 May 2023; Revised: 22 May 2023; Accepted: 27 May 2023; Published: 15 June 2023)
(Published by Research Trend)

ABSTRACT: Antimicrobial resistance is a global health challenge, prompting the search for alternative agents. The present study aims to investigate the antimicrobial activity of $MgAl_2O_4:Tb^{3+}$ nanophosphor against *E. coli, S. aureus*, and *C. albicans.* Phase formation, surface characteristics, and antimicrobial activity were analyzed by X-ray diffraction (XRD), X-ray photoelectron spectroscopy (XPS), and agar well diffusion method, respectively. XRD confirmed the successful Tb^{3+} incorporation, while XPS determined the charge states of the elements and confirmed the absence of impurities. The antibacterial studies indicate that increasing the concentration of terbium ions in the $MgAl_2O_4$ nanophosphor may further improve its antibacterial properties. While, at a concentration of 1000µg, $MgAl_2O_4:Tb^{3+}$ showed significant inhibition of the growth of tested fungal organism. Therefore, these nanophosphors may be useful in food preservation, safe cosmetics, medical devices, water treatment, etc. Future research may further optimize their efficacy, biocompatibility, and application in targeted delivery system.

Keywords: Nanophosphor, Terbium, XRD, XPS, Antimicrobial, Sol-gel combustion method.

INTRODUCTION

In recent years, nanomaterials have transformed a wide range of fields, from household products to electronics and the medical industry. Among these, spinel oxides with the AB_2O_4 structure, where A and B represent divalent and trivalent cations, respectively, and belong to the cubic space group (Fd3m), represent an important class of inorganic nanomaterials (Pratapkumar *et al.,* 2017). Their unique physical, chemical, and thermal stability make them ideal phosphors for numerous applications (Wiglusz and Grzyb 2011). $MgAl_2O_4$, a prominent member of this oxide family with a spinel crystalline structure, has garnered significant attention due to its diverse technological applications. Research shows that $MgAl_2O_4$ acts as a host for various phosphors and finds use in solid oxide fuel cells, sensors, thermoelectric devices, microwave dielectric materials, high-performance catalysts, long-lasting phosphors, X-ray imaging, light-emitting displays, and environmental monitoring (Wei *et al*., 2017).

Research has demonstrated that the incorporation of rare-earth ions (RE^{3+}) to appropriate host matrices significantly enhances their physical and chemical properties (Isha *et al.,* 2021). These rare-earth doped nanomaterials have attracted significant interest as promising phosphor materials, finding applications in modern lighting, displays, plasma display panels, forensic science, biomedical imaging, etc (Vidya and Chitra 2019; Pratapkumar *et al.,* 2017; Wiglusz and Grzyb 2011). Terbium (Tb), a member of the RE^{3+} group, has garnered significant interest because of its potential bioactivity and unique fluorescence properties (Ziqi *et al.,* 2022). Recent advancements in the use of terbium nanoparticles for applications such as tissue engineering (Natarajan *et al*., 2022), bone repair ability (Ziqi *et al*., 2022), drug delivery (Shang *et al.,* 2014), wound healing (Nethi *et al.,* 2017), and anticancer treatments (Iram *et al.,* 2016), suggest that they could play a pivotal role in the future of biomedical applications.

Further, antimicrobial resistance poses a significant global health threat, driving research efforts to identify alternative antimicrobial strategies, including antibiotic adjuvants and metal-based antimicrobial agents (Venkatesh *et al.,* 2018; Sánchez-López *et al.,* 2020). Moreover, studies have demonstrated that metal and metal oxide nanoparticles represent a novel category of materials being explored for their antimicrobial properties (Shukla, 2019; Fantozzi *et al.,* 2021; Dutta *et al*., 2021). These effects are influenced by a range of intrinsic and extrinsic factors. In addition, studies have reported the antimicrobial activity of magnesium-based nanoparticles and terbium nanoparticles against various pathogens (Fantozzi *et al.,* 2021; Kusrini *et al.,* 2023). Thus, we hypothesised that a new class of nanoparticles- Terbium doped magnesium aluminate nanophosphorsynthesized by sol-gel combustion method could effectively control pathogenic microorganism, while also developing antimicrobial compounds in an eco-friendly and sustainable manner.

MATERIALS AND METHODS

Synthesis of $MgAl_2O_4:Tb^{3+}$ nanophosphor. $MgAl_2O_4:Tb^{3+}$ nanophosphor was prepared using polymer assisted sol-gel combustion method. Stoichiometric amounts of magnesium nitrate hexahydrate ($Mg(NO_3)_2 \cdot 6H_2O$,99.99%, Sigma-Aldrich), terbium nitrate ($Tb(NO_3)_3 \cdot 6H_2O$,99.99%, Sigma-Aldrich) and aluminium nitrate nonahydrate ($Al(NO_3)_3.9H_2O$, 99.9%, Merck) were dissolved in deionized water and subjected to magnetic stirring for half an hour. To these nitrate solution appropriate amount of citric acid is added dropwise, maintaining the citrate nitrate ratio as unity. To this metal citrate complex 1 wt% polyvinylpyrrolidone (PVP) solution was added drop wise and stirring is continued for 3 h to ensure formation of the polymerised precursor. Resultant precursor was then kept in a hot air oven at 150°C for 24 hrs to obtain a yellowish dried xerogel. The dried gel is then subjected to controlled combustion at 400°C in a muffle furnace. The obtained sample is then finely ground and subjected to calcination at 900°C C/4h to obtain $MgAl_2O_4:Tb^{3+}$ nanophosphor.

Characterization. Crystal structure analysis and phase formation of the synthesized phosphors were monitored by X-ray diffraction (XRD) measurements, carried out on a Bruker (D8 ADVANCE DAVINCI) X-ray diffractometer using CuKα radiation (1.54056 Å) in the angular range (2θ) from 10°C to 70°C. X-ray photoelectron spectroscopy (XPS) measurements were carried out to analyze the surface properties and oxidation states of the elements by an X-ray photoelectron spectrometer (Thermo Scientific ESCALAB XI$^+$ A1528) integrated with AlKα (1486.6 eV) source (X-ray spot size of 900µm).

Assessment of antibacterial activity of $MgAl_2O_4:Tb^{3+}$nanophosphor. The antibacterial activity of $MgAl_2O_4:Tb^{3+}$ was carried out by the agar well diffusion method against the bacterial strains Escherichia coli (ATCC 25922) and Staphylococcus aureus (ATCC 25923) on Mueller Hinton Agar medium. Petri plates containing 20ml Mueller Hinton Agar medium were seeded with bacterial culture of E. coli and S. aureus (growth of culture adjusted according to McFarland Standard, 0.5%). Wells of approximately 10mm was bored using a well cutter and different concentrations of sample such as 250µg, 500µg and 1000µg were added. The plates were then incubated at 37°C for 24 hours. After incubation, plates were observed for the formation of clear zone around the well which corresponds to the antimicrobial activity of the sample. The inhibition zone around the well was measured in mm and recorded (NCCLS, 1993). The sample was prepared at a concentration of 50 mg/ml in dimethyl sulfoxide (DMSO). Streptomycin was used as the positive control (10 mg/ml).

Assessment of antifungal activity of $MgAl_2O_4:Tb^{3+}$ nanophosphor. Antifungal activity was determined by an agar well diffusion method against the test fungi Candida albicans using potato dextrose agar. Potato dextrose agar plates were prepared and overnight grown species of fungus, Candida albicans (ATCC 10231) were swabbed. Wells of approximately 10mm was bored using a well cutter and samples of different concentrations such as 250µg, 500µg and 1000µg were added. The zone of inhibition was measured (mm) after overnight incubation at room temperature and compared with that of standard antimycotic (Clotrimazole-10 mg/ml) (NCCLS, 1993).

RESULTS AND DISCUSSION

X-ray diffraction analysis. X-ray diffraction technique has been employed to analyse the crystallinity and phase identification of the prepared nanophosphor. Fig. 1 represents the powder x-ray diffraction pattern of the prepared sample. The pattern consists of high intensity diffraction peaks indicating high degree of crystallinity and can be well indexed according to the cubic structure of $MgAl_2O_4$ (ICDD File No. 01-070-5187, Space Group Fd-3m (227)) system. This indicates successful incorporation of Tb^{3+}ions into the $MgAl_2O_4$ host lattice and the formation of pure spinel phase $MgAl_2O_4:Tb^{3+}$nanophosphor.

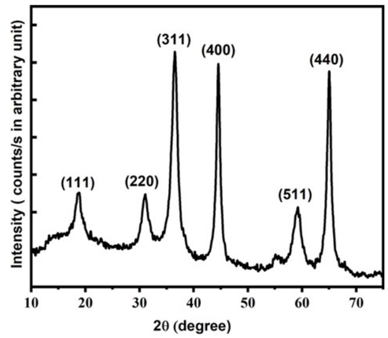

Fig. 1. X-ray diffraction pattern of $MgAl_2O_4$: Tb^{3+}nanophosphor.

The crystallite size of the sample was calculated using the Debye-Scherrer equation (Kumar *et al.,* 2016).

$$\text{Crystallite size (D)} = \frac{k\lambda}{\beta_{hkl}\cos\theta_{hkl}} \qquad (1)$$

where k is a dimensionless shape factor (= 0.9), λ is the X-ray wavelength used (CuKα =1.54056 Å), β is the full width at half the maximum intensity (FWHM) of the diffraction peaks in radian, θ is the Bragg diffraction angle and D is the crystallite size along (h k l) direction. Crystallite size evaluated by considering the prominent peaks in the XRD pattern was 9.83 nm.

XPS spectra of $MgAl_2O_4$: Tb^{3+}. X-ray photoelectron spectroscopic (XPS) measurement was carried out to gain more insight into the compositional and chemical state of $MgAl_2O_4$: Tb^{3+} sample. XPS survey spectrum shown in Fig. 2, reveal the presence of various constituents present in the synthesized nanophosphor.

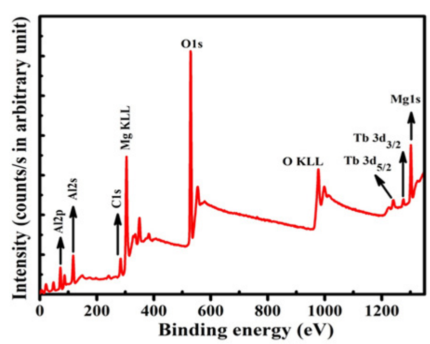

Fig. 2. XPS survey scan of $MgAl_2O_4$: Tb^{3+} nanophosphor.

The peak of adventitious carbon at 284.6 eV was taken as the reference for all charge shift corrections. The photoelectron peak observed at 1302.65 eV corresponds to the Mg^{2+} ions located at the tetrahedral sites in the spinel network and specifies the +2 oxidation states of Mg atoms present in the nanophosphor. The photoelectron peak obtained at 72.20 eV was attributed to Al-O bonds in oxide spinel structure which indicates the existence of the +3 oxidation state of aluminium in the prepared nanophosphor. The binding energy peak position of O1s bonded with Al is obtained at 529.85 which is analogous to O^{2-} ionic states of oxygen. The presence of two major peaks at 1240.19 eV and 1275.75 eV with an energy difference of 35.56 eV indicates the presence of Tb^{3+}ions in the sample (Kumar and Prakash 2020; Strohmeier, 1994; Singh *et al.,* 2015).

Antibacterial activity of $MgAl_2O_4$:Tb^{3+}. The antibacterial activity of $MgAl_2O_4$:Tb^{3+} against E. coli and S. aureus was studied and is shown in Fig. 3 a & b.

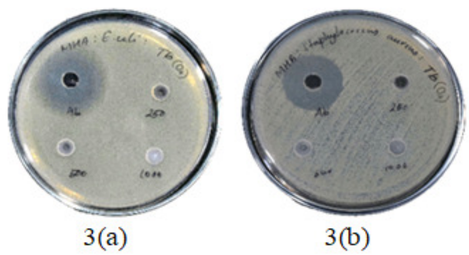

Fig. 3. The antibacterial activity of $MgAl_2O_4$:Tb^{3+} against (a) E. coli; and (b) S. aureus.

The results indicated that *E. coli* and *S. aureus* were completely resistant to $MgAl_2O_4$:Tb^{3+} which fails to show inhibition zone even at highest concentration (1000µg) (Table 1). This may be due to the reason that the concentration of the nanoparticles tested might have been too low to produce a measurable antimicrobial effect. Higher concentrations might be needed to observe an inhibition zone. Another possible explanation could be that $MgAl_2O_4$:Tb^{3+}, due to their size or properties, might not diffuse effectively through the medium, which is crucial for forming a clear zone of inhibition. Thus, we speculate that the concentration, size and distribution of terbium nanoparticle should be properly tuned to improve the antibacterial activity (Wang *et al.,* 2017).

Antifungal activity of $MgAl_2O_4$:Tb^{3+}. The highly pathogenic opportunistic fungus C. albicans was tested with different concentrations of $MgAl_2O_4$:Tb^{3+} nanophosphors (250µg, 500µg, and 1000µg). The result demonstrated that at a concentration of 1000µg, the $MgAl_2O_4$:Tb^{3+}nanophosphor exhibited an inhibition zone of 12mm against C. albicans (Fig. 4, Table 2). This observed antifungal activity may be attributed to the ability of metal oxide nanoparticles to generate reactive oxygen species (ROS), which cause oxidative damage to the cell membrane and disrupts essential biological process in the microbes, ultimately leading to cell death (Gunasekaran *et al.,* 2019).

Fig. 4. The antibacterial activity of $MgAl_2O_4$:Tb^{3+} against *C. albicans.*

Table 1: Antibacterial activity of $MgAl_2O_4$:Tb^{3+} against E. coli and S. aureus

Organism	**Zone of inhibition (mm)**			
	Streptomycin (100µg)	**$MgAl_2O_4$:Tb^{3+} (250µg)**	**$MgAl_2O_4$:Tb^{3+} (500µg)**	**$MgAl_2O_4$:Tb^{3+} (1000µg)**
E. coli	32	Nil	Nil	Nil
S. aureus	30	Nil	Nil	Nil

Table 2: **Antifungal activity of $MgAl_2O_4$:Tb^{3+} against *C. albicans*.**

Organism	**Zone of inhibition (mm)**			
	Clotrimazole (100µg)	$MgAl_2O_4$:Tb^{3+} (250µg)	$MgAl_2O_4$:Tb^{3+} (500µg)	$MgAl_2O_4$:Tb^{3+} (1000µg)
C. albicans	26	Nil	Nil	12

CONCLUSIONS

In conclusion, $MgAl_2O_4$:Tb^{3+}nanocrystals were successfully synthesized using polymer assisted sol-gel combustion method, and XRD analysis confirmed the nearly complete crystallisation of the spinel phase. XPS studies further verified the charge states of the elements in the nanophosphor. Antibacterial studies demonstrated that increasing terbium ion concentration enhances the antibacterial properties of the nanophosphors. Furthermore, antifungal studies against C. albicans showed excellent antifungal activity of $MgAl_2O_4$:Tb^{3+} nanophosphor. These findings suggest that terbium-doped $MgAl_2O_4$ have significant potential for use in antimicrobial applications. Therefore, further research could focus on optimizing these nanophosphors for practical applications in biomedicine and environmental protection.

FUTURE SCOPE

Future investigations will focus on optimizing the synthesis parameters to further improve the antimicrobial performance of $MgAl_2O_4:Tb^{3+}$ and to explore the mechanisms underlying their activity. As research progresses, the integration of terbium-based nanophosphors into medical devices and coatings may significantly reduce the risk of infections, paving the way for safer and more effective therapeutic options in healthcare.

Acknowledgement. The authors are thankful to CLIF, Trivandrum for providing XRD and XPS facilities.
Conflict of Interest. None.

REFERENCES

Dutta, P., Das, G., Boruah, S., Kumari, A., Mahanta, M., Yasin, A., Sharma, A. and Deb, L. (2021). Nanoparticles as nano priming agent for antifungal and antibacterial activity against plant pathogens. *Biological Forum-An Inernational Journal, 13*(3), 476-482.

Fantozzi, E., Rama, E., Calvio, C., Albini, B., Galinetto, P., and Bini, M. (2021). Silver Doped Magnesium Ferrite Nanoparticles: Physico-Chemical Characterization and Antibacterial Activity. *Materials (Basel), 14*(11), 2859.

Gunasekaran, S., Dinesh, A., Silambarasu, A., Thirumurugan, V. and Shankar, S. (2019). Rare Earth Element (REE) Nd^{3+} Doped CeO_2 Nanoparticles Using Aloe vera Leaf Extract: Structural, Optical and Antimicrobial Activity. *Journal of nanoscience and nanotechnology, 19*(7), 3964-3970.

Iram. S., Khan, S., Ansary, A. A., Arshad, M., Siddiqui, S., Ahmad, E., Khan, R. H. and Khan, M. S. (2016). Biogenic terbium oxide nanoparticles as the vanguard against osteosarcoma. Spectrochimica Acta Part A: *Molecular and Biomolecular Spectroscopy, 168,* 123-131.

Isha, G., Sitender, S., Shri, B. and Devender, S. (2021). Rare earth (RE) doped phosphors and their emerging applications: A review. *Ceramics International, 47 (*14), 19282-19303.

Kumar, R. G. A., Hata, S., Ikeda, K. and Gopchandran, K. G. (2016). Organic mediated synthesis of highly luminescent Li^+ ion compensated $Gd_2O_3:Eu^{3+}$ nanophosphors and their Judd–Ofelt analysis. *RSC Advances, 6*(71), 67295–67307.

Kumar, S. and Prakash, R. (2020). XPS and photoluminescence studies of Tb^{3+} doped α-Al_2O_3 phosphor. *In AIP Conference Proceedings, 2220*(1), 020019.

Kusrini, E., Safira, A. I., Usman, A., Prasetyanto, E. A., Nugrahaningtyas, K. D., Santosa, S. J. and Wilson, L. D. (2023). Nanocomposites of Terbium Sulfide Nanoparticles with a Chitosan Capping Agent for Antibacterial Applications. *Journal of Composites Science, 7* (1), 39.

Natarajan, D., Ye, Z., Wang, L., Ge, L. and Pathak, J. L. (2022). Rare earth smart nanomaterials for bone tissue engineering and implantology: Advances, challenges, and prospects. *Bioengineering & Translational Medicine, 7(*1), e10262.

National Committee for Clinical Laboratory Standards (1993a). Performance Standards for Antimicrobial Disk Susceptibility Tests—Fifth Edition: Approved Standard M2-A5. NCCLS,Villanova, PA.

Nethi, S. K., Barui, A. K., Bollu, V. S., Rao, B. R. and Patra. C. R. (2017). Pro-angiogenic Properties of Terbium Hydroxide Nanorods: Molecular Mechanisms and Therapeutic Applications in Wound Healing. *ACS Biomaterials Science & Engineering, 3*(12), 3635-3645.

Pratapkumar, C., Prashantha, S. C., Nagabhushana, H., Anilkumar, M. R., Ravikumar, C. R., Nagaswarupa, H. P. and Jnaneshwara, D. M. (2017). White light emitting magnesium aluminate nanophosphor: Near ultra violet excited photoluminescence, photometric characteristics and its UV photocatalytic activity. *Journal of Alloysand Compounds, 728,* 1124-1138.

Sánchez-López, E., Gomes, D., Esteruelas, G., Bonilla, L., Lopez-Machado, A. L., Galindo, R., Cano, A., Espina, M., Ettcheto, M., Camins, A., Silva, A. M., Durazzo, A., Santini, A., Garcia, M. L. and Souto, E. B. (2020). Metal-Based Nanoparticles as Antimicrobial Agents: An Overview. *Nanomaterials (Basel), 10*(2), 292.

Shang, H. B., Chen, F., Wu, J., Qi, C., Lu, B. Q., Chen, X. and Zhu, Y. J. (2014). Multifunctional biodegradable terbium-doped calcium phosphate nanoparticles: Facile preparation, pH-sensitive drug release and in vitro bioimaging. *RSC Advances, 4*(95), 53122-53129.

Shukla, A. K. (Ed.). (2019). Nanoparticles in Medicine. Springer Nature.

Singh, B. P., Maheshwary, M., Ramakrishna, P. V., Singh, S., Sonu, V. K., Singh, S., Singh, P., Bahadur, A., Singh, R. A. and Rai, S. B. (2015). Improved photo-luminescence behaviour of Eu^{3+} activated $CaMoO_4$ nanoparticles via Zn^{2+} incorporation. *RSC Advances, 5*(69), 55977–55985.

Strohmeier., B. (1994). Magnesium Aluminate ($MgAl_2O_4$) by XPS. *Surface Science Spectra, 3*(2), 121-127.

Venkatesh, R., Dhananjaya, N., Sateesh, M. K., Shabaaz Begum, J. P., Yashodha, S. R., Nagabhushana, H. and Shivakumara, C. (2018). Effect of Li, Na, K cations on photoluminescence of $GdAlO_3$: Eu^{3+} nanophosphor and study of Li cation on its antimicrobial activity. *Journal of Alloys and Compounds, 732,* 725-739.

Vidya, P. V. and Chitra, K. C. (2019). Irreversible histopathological modifications induced by iron oxide nanoparticles in the fish, *Oreochromis mossambicus* (Peters, 1852). *Biological Forum–An International Journal, 11*(1), 01-06.

Wang, L., Hu, C., & Shao, L. (2017). The antimicrobial activity of nanoparticles: present situation and prospects for the future. *International Journal of Nanomedicine, 12,* 1227-1249.

Wei, L., Peng, M., Tengfei, X., Jiawei, D., Yubai, P., Huamin, K. and Jiang, L. (2017). Fabrication and spectroscopic properties of $Co:MgAl_2O_4$ transparent ceramics by the HIP post-treatment. *Optical Materials, 69,* 152-157.

Wiglusz, R. J. and Grzyb, T. (2011). The effect of Tb^{3+} doping on the structure and spectroscopic properties of $MgAl_2O_4$ nanopowders. *Optical Materials, 33*(10), 1506-1513.

Ziqi, L., Yang, Y., Wenyan, K., Faming, C., Fuhua, Y., Baojin, M. and Shaohua, G. (2022). Self-assembled terbium-amino acid nanoparticles as a model for terbium biosafety and bone repair ability assessment. *Composites Part B: Engineering, 244,* 110186.

How to cite this article: Deepa Rani S., Sajan P. Shamsudeen and Abhilash Kumar R.G. (2023). Studies on the Structure and Antimicrobial Activity of $MgAl_2O_4:Tb^{3+}$ Nanophosphors Synthesized by Polymerised Sol-gel Method. *Biological Forum – An International Journal, 15*(6): 939-942.